Late-time particle emission from laser-produced graphite plasma

S. S. Harilal,[a] A. Hassanein, and M. Polek
School of Nuclear Engineering, Center for Materials Under Extreme Environment, Purdue University, West Lafayette, Indiana 47907, USA

(Received 19 June 2011; accepted 28 July 2011; published online 6 September 2011)

We report a late-time "fireworks-like" particle emission from laser-produced graphite plasma during its evolution. Plasmas were produced using graphite targets excited with 1064 nm Nd: yttrium aluminum garnet (YAG) laser in vacuum. The time evolution of graphite plasma was investigated using fast gated imaging and visible emission spectroscopy. The emission dynamics of plasma is rapidly changing with time and the delayed firework-like emission from the graphite target followed a black-body curve. Our studies indicated that such firework-like emission is strongly depended on target material properties and explained due to material spallation caused by overheating the trapped gases through thermal diffusion along the layer structures of graphite. © *2011 American Institute of Physics*. [doi:10.1063/1.3631789]

I. INTRODUCTION

Laser-produced plasma (LPP) is a highly transient phenomenon that has been the subject of considerable investigation in recent times for a multitude of applications such as extreme ultraviolet lithography light source, cellular microsurgery, laser-induced breakdown spectroscopy (LIBS), pulsed laser deposition (PLD), nanocluster, and nanotube production, sample introduction in inductively coupled plasma mass spectrometry (ICP-MS), etc. Basic understanding of plasma emission, expansion, and kinetic properties of the ejected particles is essential for all applications of LPP.[1–7] Moreover, effective control or mitigation of particle and droplet emission from LPPs is utmost important. For example, in laser plasma source applications all particle debris coming out from the plume should be mitigated and various mitigation techniques have been employed.[8] In PLD, it is a serious disadvantageous that many micron sized particles deposited together with ablated species and many methods have been tried to develop droplet free thin films.[9] It is ideal to have uniform particle distribution in laser-ablation sample introduction system for ICP-MS for avoiding elemental fractionation.[10] So understanding the particle emission and its generation during laser ablation is significantly important for LPP applications.

Recently, laser ablation of carbon has been extensively used for the deposition of diamond-like carbon (DLC) thin films[4,11] and for the production of carbon clusters.[6,12] Laser-produced carbon containing plasma emits a strong line in the water-window spectral region and hence can also be used as a light source for microscopy.[13] Carbon clusters like C_{60} and higher fullerenes are well known to be formed as a product of laser ablation of carbon in an ambient helium atmosphere.[12,14] However, the underlying physics and chemistry of processes such as carbon cluster formation or their dissociation are less than well understood. The biggest intriguing question is when and where these clusters are formed during expansive cooling of laser ablated plasma.[15,16] Hence, a fundamental understanding of the lifecycle of carbon plasma is important for improving the understanding of carbon nanostructures production and other applications of laser-produced carbon plasma. Furthermore, in the design of Tokamaks for nuclear fusion, graphite has been proposed as a material for plasma-facing components (PFCs).[17,18] Under fusion conditions, however, PFCs may encounter extremely high energy fluxes during plasma instabilities;[19] therefore, it is useful to have a thorough understanding of how graphite behaves under extreme conditions.

While much effort has been expended to characterize the laser ablation of graphite through the investigation of emission spectra, a thorough understanding of the entire laser-plasma lifecycle is lacking. Moreover, most of the previous studies focused on the earliest time of plasma evolution (<10 μs).[4,5,7,15,20–23] In this article, we report the investigation of the entire life-cycle of the laser-produced carbon plasma using imaging and spectroscopic analysis. We specifically focus on a late-time (>5 μs) arrival of firework-like particle emission from the laser generated graphite plasma.

II. EXPERIMENTAL

The experimental set-up used for the present study is similar to the one described elsewhere.[1] The plasma was generated by laser ablation of the high purity graphite sample using 1064 nm radiation pulses from a Q-switched Nd:YAG laser (full width half maximum 6 ns) in vacuum with a base pressure of 10^{-6} Torr. The incident laser power density was 5×10^{10} W/cm^2 for a spot size of approximately 200 μm. To avoid the effect of plasma confinement inside the laser produced craters, the target was translated to provide a fresh surface for each shot. An intensified charge-coupled device (ICCD) was used both individually to image the plasma and coupled to a 0.5 m spectrograph to perform spectroscopy on the plasma. The spectrograph was also equipped with a photomultiplier tube (PMT, rise time 1 ns) so that it can be used as a monochromator and in conjunction with an oscilloscope used for recording optical time of flight (OTOF). To obtain

[a]Author to whom correspondence should be addressed. Electronic mail: sharilal@purdue.edu.

kinetic profiles of the ionic species, a Faraday cup (FC) was employed. Using these diagnostics, it was possible to obtain a comprehensive picture of the complete time-evolution of the LPP.

III. RESULTS AND DISCUSSIONS

LPPs are typically hot and dense in the earliest time and cools rapidly with time. During the earliest time, ionic species contribute significant emission, and at later times, both neutrals and molecular species predominate. Molten droplets and particulates are also formed during violent ablation process. Fast imaging diagnostic provides details about plume expansion dynamics as well as particle emission features.[15,24] Because of the transient nature of LPP expansion, time resolved plasma diagnostics play an indispensable tool for understanding its evolution. Typically plasma emission begins on the target surface soon after the laser photons reach the surface and most of the plume emission in vacuum is concentrated at times <1 μs. However, it has been noticed that graphite plasma emit strongly at late-times. Figure 1 shows the ICCD image of graphite plasma recorded at 30 μs after the onset of plasma formation indicating strong particle emission from the target. We investigated the mechanisms that causing the firework-like emission from graphite plasma.

The emission dynamics of graphite plasma is rapidly changing with time and the delayed fireworks-like features appear around 5 μs after the onset of the plasma formation and persist for long delay times. Figure 2 shows ICCD images captured sequentially over the life-time of the plasma. The gate-width of the camera exposure was increased incrementally for each frame to compensate for the drop in emission intensity as the plasma evolves. The sequence starts with 10 ns and incrementally increased to 50 ns until 1 μs delay after the onset of plasma formation. In this regime, plasma self-emission is found to be maximum. A constant 1 μs and 10 μs gate widths are used for capturing images in the time window of 1–10 μs 10–300 μs, respectively. In the early times, normal

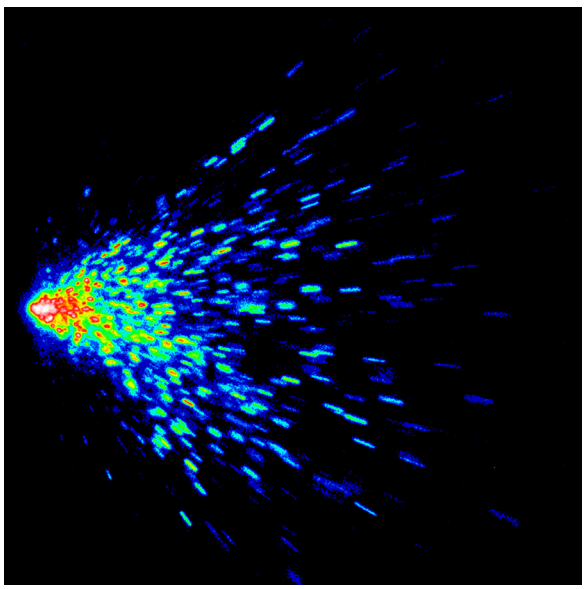

FIG. 1. (Color online) ICCD image of the graphite plume recorded at 30 μs after the onset of plasma formation.

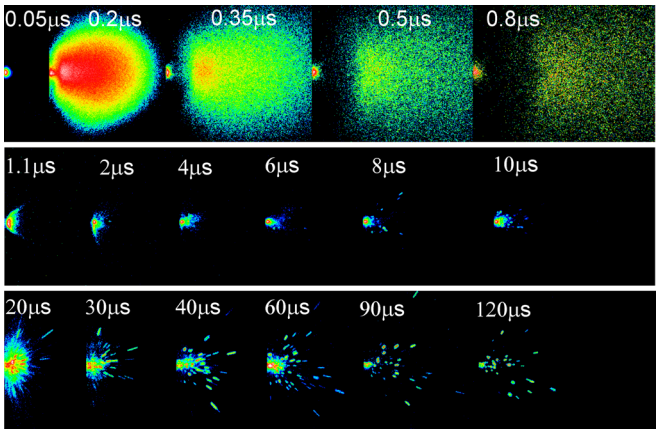

FIG. 2. (Color online) ICCD images of graphite plasma recorded at various times after the onset of plasma formation. All images were normalized to its maximum intensity for better viewpoint. The gate-width of the camera exposure was increased incrementally for each frame to compensate for the drop in emission intensity as the plasma evolves.

LPP expansion is evident, i.e., a bright spark at the onset of the plasma followed by free, adiabatic expansion and a consequent drop in intensity as the plasma disperses. Interestingly, the emission dies off after about a microsecond but there remains incandescent emission from the target. Then, after a few microseconds, fireworks-like emission is observed as slow-moving particle-like ejection from the target. The fireworks-like emission peaks around 20–30 μs after the onset of plasma. Though the plasma expands spherically at the early times, most of the delayed particle emission is concentrated within a cone angle of 35° with respect to the target normal.

We utilized optical emission spectroscopy (OES) for examining emission features of plasma at various times after the onset of plasma formation. Spectral details can also be useful for estimating the plasma ionization balance, rate processes, densities, and temperatures.[25] The recorded emission spectra at various locations of the plasma plume during a certain time after the onset of plasma formation are given in Figure 3. There are several interesting features of these plots worth noting. At early times and close to the target (e.g., 0-100 ns and 0-1 mm), intense continuum emission dominates over line emission. The continuum radiation, or bremsstrahlung, occurs when a free electron collides with another particle and makes a transition to another free state of lower energy, with the emission of photons. In sufficiently hot plasma, most of the atoms are stripped of their orbital electrons, hence making electron-ion recombination and bremsstrahlung the dominant emission mechanisms. Along with continuum, the prominent line emission noticed in the early times includes C I, C II, C III, and C IV. As the plasma evolves in time from 100 ns to 1 μs, appearance of Swan band emission from excited C_2 species is noticed along with the ionic and neutral line emission. After 1 μs, however, the line emission disappears and gives way to broadband, incandescent-like emission. The broadband emission noticed at later times corresponding to firework-like emission observed in the ICCD plume imaging. In order to accommodate less intensity of firework-like emission compared to plume emission at earlier times, a higher spectrograph slit width is used for recording the spectra.

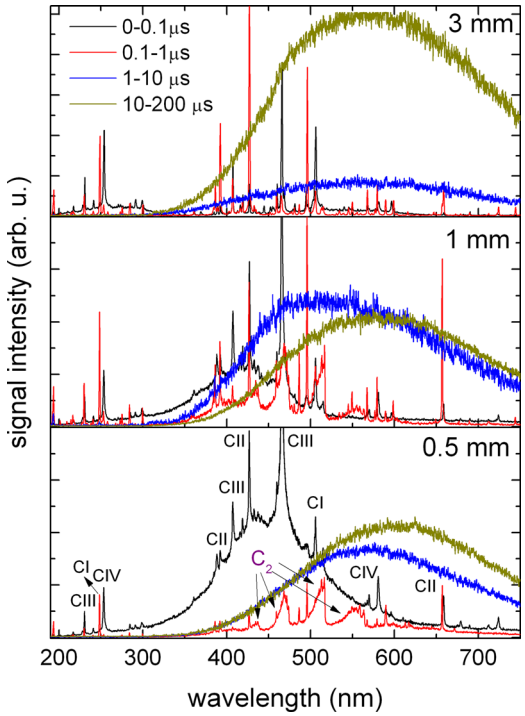

FIG. 3. (Color online) Spectra of laser produced graphite plasma at various distances (0.5 mm, 1 mm, and 3 mm), and at different time, windows after the onset of plasma formation are given. The prominent lines are marked. For recording the plume spectra, a slit width of 20 μm was used while a 50 μm slit width was used for recording the blackbody emission from late-time particles.

It is believed that molecular species in the plasma plume are formed at later time and at farther away from the target due to recombination.[23] Intriguingly, the Swan band emission is noticed only at shorter distances and peaked during 100–1000 ns time window. During 1–10 μs time domain, blackbody-type emission dominates at all distances from the target. It should be remembered that typically 1–3 μs time window is used for LIBS elemental detection.[26] However, the presence of ambient atmospheres confines the plasma plume and hence extends the life of the plasma plume, and in comparison, the present work is done in vacuum.[24,27] Based on spectroscopic results, the "fireworks-like" is due to incandescent emission from the ejected hot particles or droplets. Because, this incandescent emission peaks around 600 nm, it is possible to calculate the temperature of the emitting bodies which is approximately 5000 K.

We examined TOF of line emission from various species in the plasma to elucidate their kinetics and its relation with late time particle emission. The respective emission lines selected are C I (247.9 nm), C II (392.4 nm), C III (407.3 nm), and C_2 (516.5 nm). Typical kinetic energy profiles obtained from OTOF studies are given in Figure 4. Not surprisingly, due to space charge effects, the highly-charged ions have the largest velocity and the C_2 dimer and neutral species have the lowest velocity. However, C_2 emission is noticed only at early times and not evident at later times. The maximum probable kinetic energies measured for each species in the plasma are 8 eV, 54 eV, 133 eV, and 776 eV, respectively, for C_2, C I, C II, and C III. For comparison, the ionic profiles recorded using a FC positioned at 16 cm away

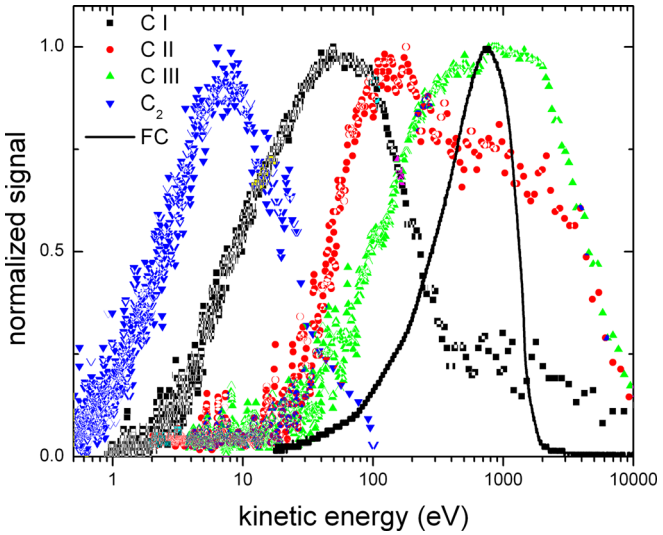

FIG. 4. (Color online) Kinetic energy profiles of various species in the plasma recorded at 2 mm from the target surface. The emission lines selected for these studies are C I (247.9 nm), C II (392.4 nm), C III (407.3 nm), and C_2 (517.6 nm). The solid curve represents the KE profile obtained from FC ion signal.

from target and 15° with respect to the target normal is also given in Figure 4. The kinetic energy spectrum of ionic species is found to be narrower compared to OTOF profiles. This could be due to smaller solid angle collection of the ions using FC compared to line-of-sight collection used in the OTOF and difference in collection angle.

We have also examined the TOF of fireworks-like emission. For this purpose, we collected the temporal profile of the incandescent emission at 550 nm and it is given in Figure 5. The temporal profile shows the incandescent emission peaks around 20 μs after the onset of plasma formation which is consistent with our ICCD images. The emission profiles also showing spikes in the decay. This could be understood by evaluating the ICCD images: this fireworks-like emission process is very sporadic in nature. The velocity of the ejected particles $\sim 5 \times 10^3$ cm/s, which is more than two orders, is slower than the velocities of other species in the plasma

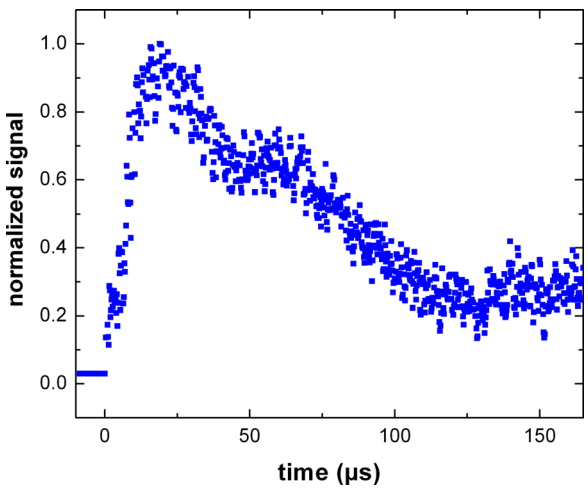

FIG. 5. (Color online) The temporal profile of the incandescent emission recorded at 1 mm from the target surface.

plume. The estimated the velocity of the particles from the streaks seen in the ICCD images gave similar velocity values obtained using OTOF technique.

OTOF studies indicate that firework-like emission noticed at later times probably coming from heavy particles. Transient melting and ejection of particles during laser ablation strongly affect the ablation efficiency as well as deleterious effects for using laser ablation in ICP-MS sample introduction, thin film preparation, and micromaching. It is well known that carbon clusters like fullerenes are formed during laser ablation of carbon by chaining the C_2 molecules in the plasma.[14] There are two mechanisms that could exist for the particle formation during the laser ablation of carbon, viz. dissociative and recombinational. According to Iida *et al.*,[28] at low laser irradiance levels, graphite will be ablated layer by layer producing large particles, and the dominant mechanism for the production of C_2 emission is the electron collision with C_n cations and neutrals ($n > 2$), while at high irradiance levels, C_2 formation is mainly due to electron-ion and ion-ion recombination. Our spectroscopic emission diagnostics showed that most of the C_2 Swan band emission appeared closer to the target and at earliest time. Hence, we rule out the role of C_2 for the occurrence of the fireworks-like emission noticed at the later time. This fact is also supported by the observed kinetics of C_2 species and late time emitted particles using OTOF. Hence, the formation of the particles noticed at late times is not related to plume species.

We further investigated the effect of target material property and laser intensity on fireworks-like emission. Among the targets used in our experiments (Al, Cu, Sn, W, and C), graphite is the only target material that showed such delayed emission. The delayed emission was also seen at a wide range of laser intensities ($1–10^3$ GW/cm^2) studied using 1064 nm laser excitation and showed no intensity threshold dependence. These results indicate that the observed property is more material specific rather than laser irradiation conditions.

Some of the possible mechanisms leading to particle-emission during laser ablation process are phase explosion and spallation and both these processes are taking place in the same time domain and are closely linked with each other.[29–31] Experimental observations of onset of the ejection of liquid droplets as well as a steep increase in ablation rate are often interpreted as evidence of phase explosion during laser ablation.[30,32] The material ejection in phase explosion is due to an explosive decomposition of the target material superheated beyond the limit of thermodynamic stability into a two-phase mixture of liquid and vapor. From the kinetic energy profiles obtained from FC, we estimated the average ionization state of the plasma from the following equation:[33] $E = 5(Z+1) \times T_e$ where E is the most probable kinetic energy of ions in the plasma and Z is the average ionization state. Previous investigations under identical experimental conditions provided the necessary temperature and density measurements of the graphite plasma for these calculations.[34] In this case, the average ionization state in the plasma is found to be approximately 3 (at the earliest time) which can in turn be used to calculate the pressure created by the plasma plume from the ideal gas law: $P = n(Z+1)kT$. At the onset, the temperature (~20 eV) and pressure (~13 GPa) of the plasma allow for the liquid phase to be present. During this time, it is likely that liquid droplets are ejected from the target. Within 100 ns, the pressure of the plasma drops to 1 MPa, and after 1 μs, the pressure drops to 100 kPa. The phase diagram of graphite clearly shows that, in the time regime of the "fire-works," the pressure exerted by the plasma is insufficient to allow for liquid droplets. According to the phase diagram, in the tens to hundreds of kPa pressure regime and 5000 K temperature regime, the carbon must be in the gaseous phase.[35] As the carbon cools, it skips the liquid phase and simply adsorbs to form solid graphite particles. This again suggests that these fireworks are actually incandescently glowing graphite soot particles and not droplets of molten graphite. It rules out phase explosion for the observation of fireworks-like emission at later times of plasma evolution. In spallation, the compressive stresses induced by the laser leads to mechanical fracture of the solid material and sputtering of melted layer. Typically, laser intensities required for spallation are significantly lower than the ones involved for explosive boiling.[31]

Our results clearly indicate that the late-time particle emission is more related target material than the incidental laser parameters. So, the reasoning of the particle emission at delayed times could not be related to both photomechanical effect and phase explosion. The graphite usually has layered structure with inter-layer spacing of fraction of nm where atoms were arranged in a hexagonal lattice.[36] The thermal conductivity of graphite is very high along the ab direction (parallel to the layers) while it is approximately 200 times lower in the direction perpendicular to ab plane (c direction, bulk).[35] Hence, graphite is a very good conductor along the lattice plane and a good thermal insulator in the other direction. Moreover, it is known that the different graphites can contain significantly different amounts of physically and chemically adsorbed gas impurities in between the layers. The gas impurities in the target material eventually get heated up during plasma formation and along with decrease in heat transfer between the laser heated zone and bulk target. As time evolves, the heated trapped gas layers reach very high pressure leading to particle emission at the later times. This also explains the delayed emission from simple estimates of heat diffusion time needed to cross the grain and heat the trapped gases in between. This is also supported by the fact that we noticed similar fireworks-like emission with pyrolytic graphite though with much less intense due to the fine and dense structure of pyrolytic graphite with very little trapped gases in between. Such structure resembles metallic targets which did not exhibit fireworks-like explosive emission which further endorse our concept.

Similar firework-like particle emission was noticed previously in carbon based materials during intense transient heat loads generated by electron beams and explained as brittle destruction[37–39] as well as during erosion of graphite by pulsed arc discharges.[40] In electron beam heated experiments, large particle release from graphite was significantly enhanced at elevated temperatures indicating there is a threshold temperature for particle release.[37] Carbon based materials have been used successfully in most of the present day tokamak and stellarator experiments worldwide due to

its attractive properties like excellent thermal conductivity, favorable mechanical properties, and a good plasma compatibility. However, the generation of dust particles due to brittle destruction observed during Tokamak operation or in severe thermal shock experiments, arouse critical safety issue in future fusion devices.[41,42]

IV. CONCLUSIONS

We investigated the dynamics of particle emission from laser-produced graphite plasma using fast-gated imaging and spectroscopic diagnostics. In the imaging studies, a curious fireworks-like emission was noticed well after the emission from the LPP had died out. Spectroscopic studies showed the late time firework is represented by a Planckian curve with a temperature ~5000 K and its kinetics are not related to dynamics of plume species. Our results indicate that the fireworks are slow-moving, incandescently glowing solid particles of graphite being ejected from the target at later times. The carbon soot emission at later stages of lifecycle is explained due to material spallation caused by overheating the trapped gases through thermal diffusion along the layer structures of graphite.

ACKNOWLEDGMENTS

The authors thank David Campos for experimental help. This work is supported by US DOE NNSA (Contract No. DE-NA0000463).

[1]D. Campos, S. S. Harilal, and A. Hassanein, J. Appl. Phys. **108**, 113305 (2010).
[2]D. B. Chrisey and G. K. Hubler, *Pulsed Laser Deposition of Thin Films* (Wiley, New York, 1994).
[3]S. S. Harilal, T. Sizyuk, A. Hassanein, D. Campos, P. Hough, and V. Sizyuk, J. Appl. Phys. **109**, 063306 (2011).
[4]J. Haverkamp, R. M. Mayo, M. A. Bourham, J. Narayan, C. Jin, and G. Duscher, J. Appl. Phys. **93**, 3627 (2003).
[5]A. Kushwaha, A. Mohanta, and R. K. Thareja, J. Appl. Phys. **105**, 044902 (2009).
[6]D. E. Motaung, M. K. Moodley, E. Manikandan, and N. J. Coville, J. Appl. Phys. **107**, 044308 (2010).
[7]D. Yadav, V. Gupta, and R. K. Thareja, J. Appl. Phys. **106**, 064903 (2009).
[8]S. S. Harilal, B. O'shay, Y. Tao, and M. S. Tillack, Appl. Phys. B **86**, 547 (2007).
[9]H. Minami, D. Manage, Y. Y. Tsui, M. Malac, and R. Egerton, Appl. Phys. A **73**, 531 (2001).
[10]J. Koch and D. Guenther, Appl. Spectrosc. **65**, 155A (2011).
[11]A. A. Voevodin and M. S. Donley, Surf. Coat. Technol. **82**, 199 (1996).
[12]E. A. Rohlfing, J. Chem. Phys. **89**, 6103 (1988).
[13]J. de Groot, O. Hemberg, A. Holmberg, and H. M. Hertz, J. Appl. Phys. **94**, 3717 (2003).
[14]H. W. Kroto, J. R. Heath, S. C. Obrien, R. F. Curl, and R. E. Smalley, Nature (London) **318**, 162 (1985).
[15]K. F. Al-Shboul, S. S. Harilal, A. Hassanein, and M. Polek, J. Appl. Phys. **109**, 053302 (2011).
[16]M. K. Moodley and N. J. Coville, Chem. Phys. Lett. **498**, 140 (2010).
[17]S. S. Harilal, J. P. Allain, A. Hassanein, M. R. Hendricks, and M. Nieto-Perez, Appl. Surf. Sci. **255**, 8539 (2009).
[18]Y. Hirooka, R. Conn, R. Causey, D. Croessmann, R. Doerner, D. Holland, M. Khandagle, T. Matsuda, G. Smolik, T. Sogabe, J. Whitley, and K. Wilson, J. Nucl. Mater. **176**, 473 (1990).
[19]A. Hassanein and I. Konkashbaev, J. Nucl. Mater. **290**, 1074 (2001).
[20]C. S. Ake, R. S. de Castro, H. Sobral, and M. Villagran-Muniz, J. Appl. Phys. **100**, 053305 (2006).
[21]J. J. Camacho, L. Diaz, M. Santos, L. J. Juan, and J. M. L. Poyato, J. Appl. Phys. **106**, 033306 (2009).
[22]S. S. Harilal, R. C. Issac, C. V. Bindhu, V. P. N. Nampoori, and C. P. G. Vallabhan, J. Appl. Phys. **81**, 3637 (1997).
[23]Y. Yamagata, A. Sharma, J. Narayan, R. M. Mayo, J. W. Newman, and K. Ebihara, J. Appl. Phys. **88**, 6861 (2000).
[24]S. S. Harilal, C. V. Bindhu, M. S. Tillack, F. Najmabadi, and A. C. Gaeris, J. Appl. Phys. **93**, 2380 (2003).
[25]D. Campos, S. S. Harilal, and A. Hassanein, Appl. Phys. Lett. **96**, 151501 (2010).
[26]A. W. Miziolek, V. Palleschi, and I. Schechter, *LIBS Fundamentals and Applications* (Cambridge University Press, New York, 2008).
[27]S. S. Harilal, B. O'shay, Y. Tao, and M. S. Tillack, J. Appl. Phys. **99**, 083303 (2006).
[28]Y. Iida and E. S. Yeung, Appl. Spectrosc. **48**, 945 (1994).
[29]A. A. Ionin, S. I. Kudryashov, and L. V. Seleznev, Phys. Rev. E **82**, 016404 (2010).
[30]C. Porneala and D. A. Willis, Appl. Phys. Lett. **89**, 211121 (2006).
[31]L. V. Zhigilei, Z. B. Lin, and D. S. Ivanov, J. Phys. Chem. **113**, 11892 (2009).
[32]J. H. Yoo, S. H. Jeong, X. L. Mao, R. Greif, and R. E. Russo, Appl. Phys. Lett. **76**, 783 (2000).
[33]P. T. Rumsby and J. W. M. Paul, Plasma Phys. Control. Fusion **16**, 247 (1974).
[34]S. S. Harilal, C. V. Bindhu, R. C. Issac, V. P. N. Nampoori, and C. P. G. Vallabhan, J. Appl. Phys. **82**, 2140 (1997).
[35]H. O. Pierson, *Handbook of Carbon, Graphite, Diamonds and Fullerenes: Processing, Properties and Applications* (Noyes, NJ, 1993).
[36]B. Partoens and F. M. Peeters, Phys. Rev. B **74**, 075404 (2006).
[37]T. Hirai, S. Brezinsek, W. Kuehnlein, J. Linke, and G. Sergienko, Phys. Scr. **T111**, 163 (2004).
[38]J. Linke, M. Rubel, J. A. Malmberg, J. R. Drake, R. Duwe, H. J. Penkalla, M. Rodig, and E. Wessel, Phys. Scr. **T91**, 36 (2001).
[39]H. Bolt, J. Linke, H. J. Penkalla, and E. Tarret, Phys. Scr. **T81**, 94 (1999).
[40]T. Schulke and A. Anders, Plas. Sour. Sci. Technol. **8**, 567 (1999).
[41]T. Burtseva, A. Hassanein, I. Ovchinnikov, and V. Titov, J. Nucl. Mater. **290**, 1059 (2001).
[42]J. Winter, Phys. Plasmas **7**, 3862 (2000).